DSN Microwave Antenna Holography Part II: Data Processing and Display of High-Resolution Effective Maps

D. J. Rochblatt
Radio Frequency and Microwave Subsystems Section

Y. Rahmat-Samii and J. H. Mumford
Spacecraft Telecommunications Equipment Section

This article presents the results of a recently completed computer graphic package for the process and display of holographically recorded data into effective aperture maps. The term "effective maps" (labelled "provisional" on the holograms) signifies that the maps include contributions of surface mechanical errors as well as other electromagnetic factors (phase error due to feed/subreflector misalignment, linear phase error contribution due to pointing errors, subreflector flange diffraction effects, and strut diffraction shadows). While these maps do not show the true mechanical surface errors, they nevertheless show the equivalent errors, which are effective in determining overall antenna performance. Final steps to remove electromagnetic pointing and misalignment factors are now in progress. The processing and display of high-resolution effective maps of a 64m antenna (DSS 63) are presented.

I. Introduction

The fundamentals of the microwave holography technique have been presented by Rahmat-Samii in Refs. 1 and 2, to which the reader is referred for details on mathematical formulations, numerical simulations, application of an iterative algorithm, etc. Additionally, the basic principles of the measurement aspects have been outlined in an earlier TDA Progress Report (Ref. 3), which is considered as Part I of this article. Microwave holography is expected to be a key technique for achieving outstanding DSN 8.4-GHz performance and enabling future DSN capability at even shorter wavelength, such as the 32/34-GHz bands recently allocated for deep space telemetry.

The NASA Deep Space Network is currently upgrading its three 64m antennas to 70m to achieve a microwave gain increase of 1.9 dB at 8.4 GHz (X-band). This performance improvement is applicable to all future deep space missions and to solar system radar, as well as to more immediate support for the 1989 Voyager 2 encounter with Neptune. The precise alignment of the reflector panels and precise location of the subreflector are the final key factors in achieving the 1.9-dB gain increase at X-band, and are essential for future acceptable performance at 32 GHz.

More than 3800 m^2 of area is associated with each 70m antenna, comprising 1272 individual panels and 5472 adjusters.

These panels must be aligned to a precision of 0.25-mm (0.01-in.) rms. In the past, antenna panel alignment was accomplished using optical (theodolite) techniques. These techniques will still be used to provide an initial surface accuracy, but to achieve the final precise panel alignment and precise subreflector position, the microwave holography technique will be applied to advantage (Refs. 1 and 2).

Holography, "total recording," acquires phase and amplitude raster-scan patterns of the antenna far-field angular response (Refs. 1 through 3). The holography metrology is based on interferometrically connecting a reference antenna to the large test antenna and digitally recording the test antenna amplitude and phase response. This is done by continuously scanning the test antenna against a geosynchronous satellite, following a two-dimensional grid. The angular extent (or number of sidelobes) of the response that must be acquired is inversely proportional to the size of the desired resolution cell in the processed holographic maps (Ref. 1). At 11.45-GHz measurement frequency, resolution cells of 0.4m diameter have been achieved, providing several resolution cells per individual reflecting panel. An Inverse Fast Fourier Transform (IFFT) algorithm is then used to obtain the desired information, consisting of the test antenna aperture amplitude and phase response (Ref. 1). From the aperture phase response, the "surface error map" is calculated; the amplitude response ("surface current map") is directly displayed. It is the information in the "surface error map" that is used to calculate the adjustments of the individual panels in an overall main reflector best-fit reference frame. The "surface current map" provides valuable information about the energy pattern distribution in the antenna aperture. JPL engineering has developed the data processing and display capability to produce "effective maps" on a portable HP-1000 computer. The short-term goal is to develop a capability to display a "final map" and panel adjustment correction listing. Thus far, a contractor (Eikontech, Ltd.) has supplied the digitized raw data of the test antenna far-field amplitude and phase response. The long-term goal is to develop (or acquire) the data recording as well as processing and display capability.

II. High-Resolution Test Results

Figures 1 and 2 are black-and-white presentations of the 14-color computer displays of effective maps of the DSS 63 64m antenna. (The color version may be ordered from the JPL Photo Lab. Reprint order numbers for Figures 1 and 2 are JPL 248AC and JPL 248BC, respectively.) The holography measurement was made at 11.451 GHz, using the linearly polarized beacon from geosynchronous orbit satellite ECS-1 as the illumination source. The satellite was positioned 13° east of Greenwich. At DSS 63, this satellite appears at elevation 40.2 degrees, azimuth 154.4 degrees. Its diurnal motion was less than ±0.1 degrees in elevation and azimuth at the time of the tests. The e.i.r.p. of the ECS-1 beacon is 11 dBW. With the receiver bandwidth of 2.5 Hz, this provided a beam peak signal-to-noise ratio of 73 dB. The panels of the 64m DSS 63 antenna typically measure about 3.5m × 1.5m. In order to determine the mean position and tilt of the panels, it is necessary for the resolution of the holography images to be at least as small as half the smallest panel dimension (Ref. 2). By recording a data array of 189 × 189, a resolution of 0.4m was achieved. The duration of the measurement was about 11 hours (Ref. 4).

The raw data, supplied to JPL by Eikontech, Ltd. was taken on 28 May 1985. The contractor corrected the recorded data for satellite motion, phase drift, pointing offset errors, baseline phase errors, and azimuth/elevation to rectangular u,v coordinate interpolation.

The digitized data array (far-field response) of 189 × 189 complex numbers (32 bits each for real and imaginary parts) was extended with zeros at the prescribed Δu, Δv intervals to a 256 × 256 array and processed by the IFFT program. The result, the near-field aperture response of the antenna, was then further processed to display two effective maps: effective surface error map (derived from phase) and surface current map (amplitude). The complete processing and display cycle with no iteration took about 90 minutes. Before panel correction adjustment can be calculated, the data (of future "final" maps) must be fitted globally to the "best" parabola (a criteria that must be determined) and then locally best-fitted to determine panel screw point adjustments (finite element models including girders, beams, and panel skins are included in the software).

Damaged and locally misaligned panels can clearly be observed on the surface error map (especially on the color images). For example, the panel close to the lower right strut appears depressed (this panel suffered accidental damage during an earlier modification). Other grossly misaligned panels can clearly be observed.

Diffraction effects due to subreflector flange appear as exceptionally well-defined concentric rings close to the edge of the dish on both maps. Figures 3 and 4 show that independent computer simulation/analysis predictions of the aperture functions corresponding to Figures 1 and 2 agree well in describing the subreflector flange diffraction effect. The subreflector flange was designed for optimum 2295-MHz beam shaping (Figure 5, from Ref. 5).

Panel grids, subreflector blockage, quadripod blockage, and projected shadows have been intentionally overlayed on the "surface error map," while only direct (plane wave) optical

shadows have been overlayed on the "surface current map." Spherical wave-shadowed regions of the surface error map generally contain meaningless phase information (the shadowed panels cannot be set from these data) and are therefore suppressed. The same regions of the surface current map are displayed, as valuable information can be gained from the shadow details.

III. Summary

A key benefit of the microwave holography technique is that the mathematically transformed data contain information about the antenna beam formation, allowing precise knowledge not only about the detailed panel alignments on a "local" scale, but also, importantly, about the subreflector alignment on a "global" scale.

Considerable further detailed work is required to achieve full data reduction, analysis, and manipulation, and improved display capability. However, the fundamentals are now in place and operating. Work is needed to produce a more complete analysis capability and toward better understanding via computer simulation of the various error types (random noise, ordered pointing errors, subreflector/horn misalignments) and examination of needs at 32 GHz. Following completion of that work, attention needs to shift toward data acquisition capability.

Acknowledgments

The authors wish to thank Boris Seidel, who contracted and supervised the supplying of the raw data used to produce the holography maps in this report, and Dan Bathker for his numerous helpful technical discussions.

References

1. Rahmat-Samii, Y., "Surface Diagnosis of Large Reflector Antennas using Microwave Holographic Metrology: An Iterative Approach," *Radio Science*, Vol. 19, No. 5, pp. 1205–1217, Sept.–Oct., 1984.

2. Rahmat-Samii, Y., "Microwave Holography of Large Reflector Antennas: Simulation Algorithms," *IEEE Transaction on AP*, Vol. AP-33, No. 11, pp. 1174–1203, November 1985.

3. Rochblatt, D. J., and Seidel, B. L., "DSN Microwave Antenna Holography," *TDA Progress Report 42-76*, pp. 27–34, October–December, 1983.

4. Godwin, M. P., Schoessow, E. P., and Richards, P. J., "Final Report on Holographic Tests at S-band and K-band on the DSS-63 64-Meter Antenna," prepared for the Jet Propulsion Laboratory under Contract No. 956984, February 1986.

5. Bathker, D. A., "Radio Frequency Performance of a 210-ft Ground Antenna, X-band," JPL Technical Report 32-1417, Jet Propulsion Laboratory, December 15, 1969.

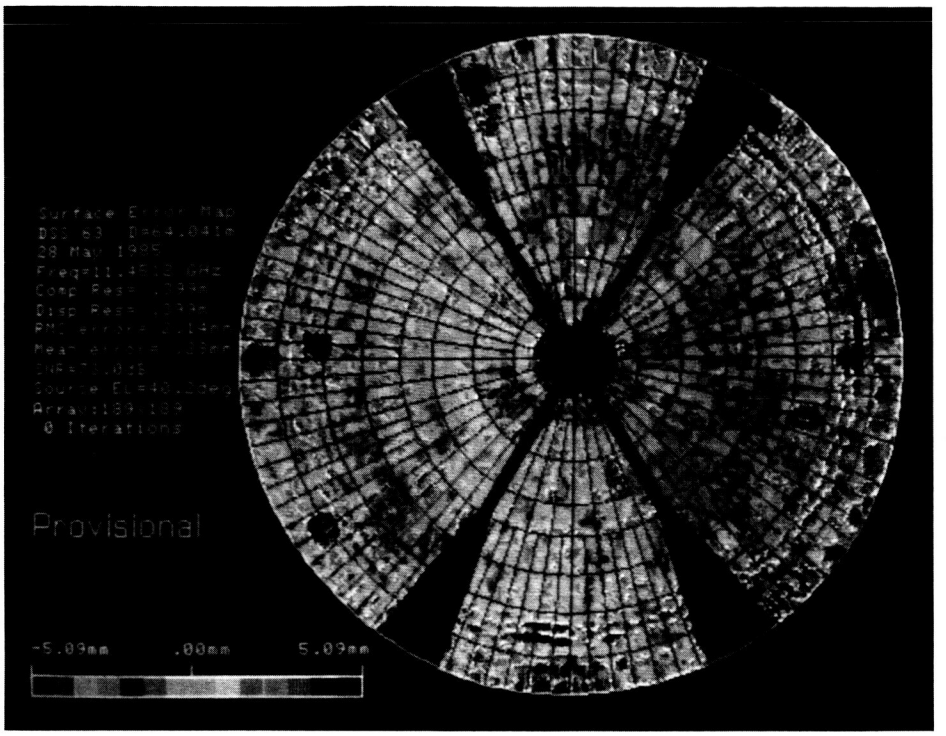

Fig. 1. DSS 63 64-m effective surface error map

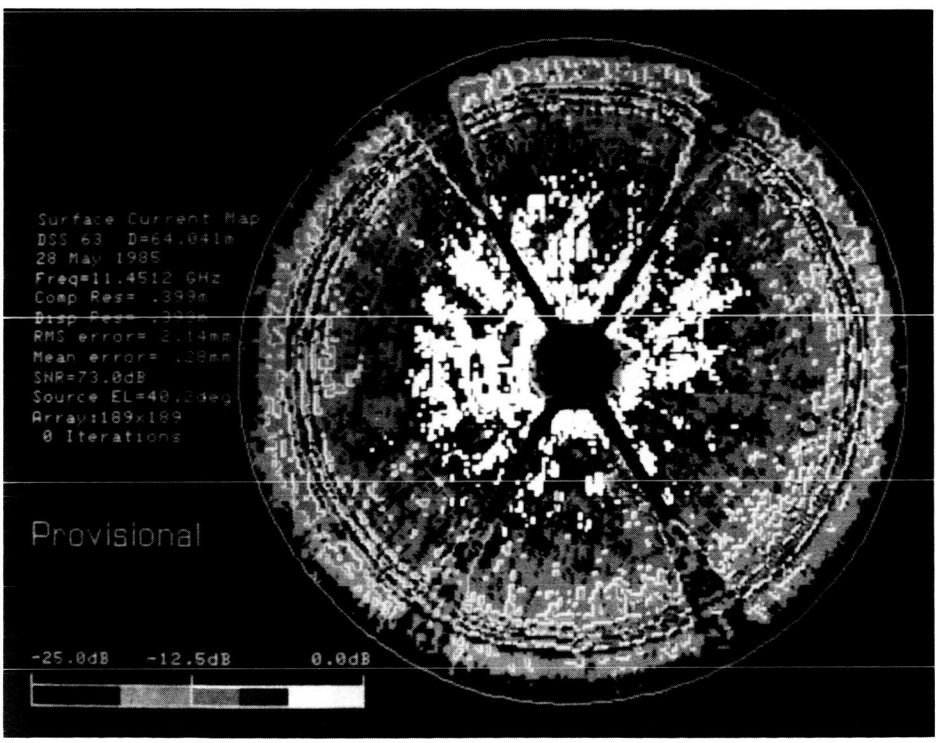

Fig. 2. DSS 63 64-m effective surface current map

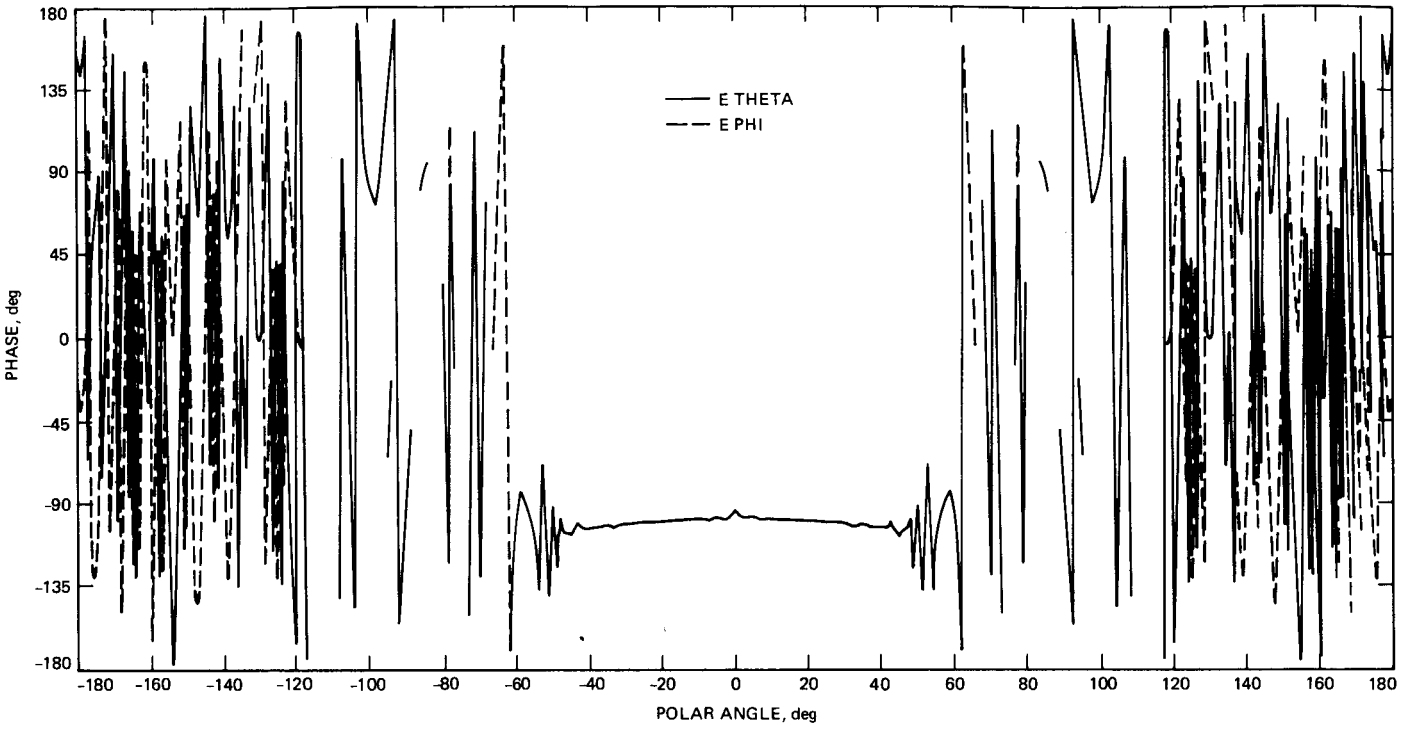

Fig. 3. Subreflector scattered radiation patterns, phase

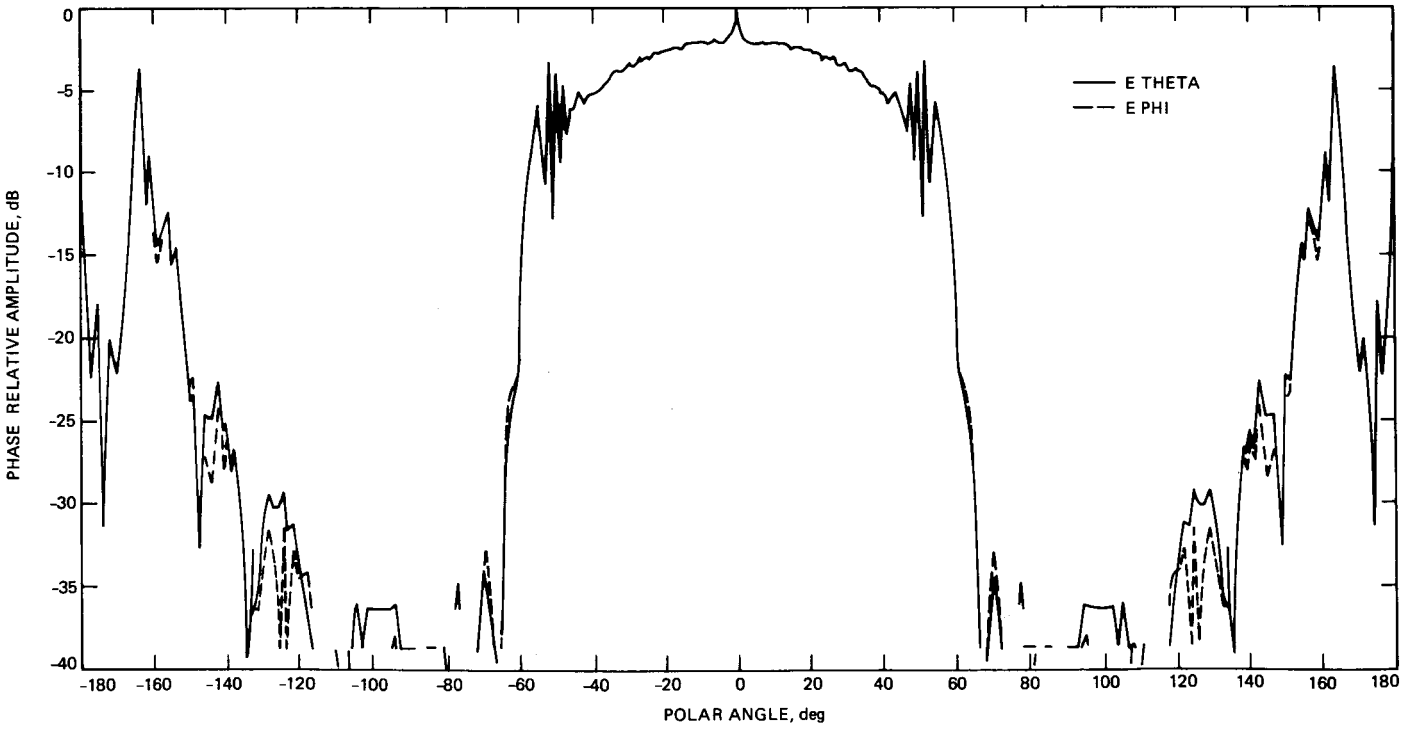

Fig. 4. Subreflector scattered radiation patterns, amplitude

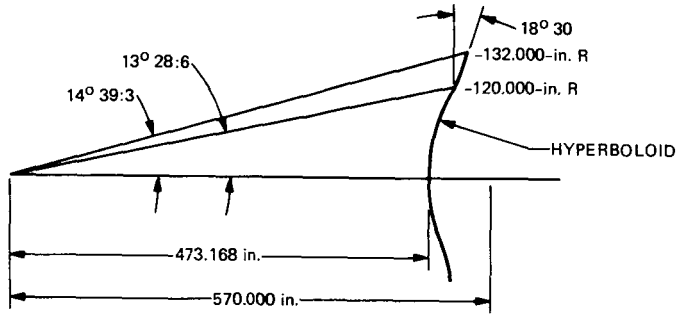

Fig. 5. 64-m subreflector configuration